1 ***Quality control and monitoring of NSM CFRP systems: E-modulus***

2 ***evolution of epoxy adhesive and its relation to the pull-out force***

3

4 Pedro Fernandes[a], José L. Granja[a], Andrea Benedetti[a], José Sena-Cruz[a][1], Miguel Azenha[a]

5 [a] ISISE – Institute for Sustainability and Innovation in Structural Engineering

6 University of Minho, School of Engineering

7 Department of Civil Engineering

8 Campus de Azurém

9 4800-058 Guimarães

10 Portugal

11 Tel: +351 253 510 200; Fax: +351 253 510 217

12

13 **ABSTRACT**

14 The present paper describes the application of an innovative technique (termed EMM-ARM:

15 Elasticity Modulus Monitoring through Ambient Response Method) for continuous monitoring

16 of the stiffening process of an epoxy adhesive used in near-surface mounted (NSM) fibre

17 reinforced polymer (FRP) reinforcements. A simultaneous study of direct pull-out tests with

18 concrete specimens strengthened with NSM carbon FRP laminate strips was carried out to

19 compare the evolution of bond performance with the E-modulus of epoxy since early ages. A

20 relationship between the evolution of epoxy E-modulus and the maximum pull-out force is

21 assessed, highlighting the potential of applying EMM-ARM for quality control and decision-

22 making assistance of NSM systems.

23

24 **KEYWORDS**

25 A. Carbon fibre

26 A. Thermosetting resin

[1] Corresponding author: jsena@civil.uminho.pt

1   B. Cure behaviour

2   D. Non-destructive testing

3   Near-surface mounted reinforcement

1   INTRODUCTION

Strengthening of reinforced concrete (RC) members with externally bonded fibre-reinforced polymer (FRP) laminates has become a popular technique over the past two decades [1, 2]. More recently, the near-surface mounted (NSM) strengthening technique using FRP has been increasingly used as an effective alternative to the classical approach of applying externally bonded FRP [3, 4]. In the NSM FRP strengthening method, FRP bars are inserted into pre-cut grooves opened in the concrete cover of the elements to be strengthened. The FRP reinforcement is bonded to concrete with an appropriate groove filler, typically an epoxy adhesive [3]. This technique provides the FRP bars with protecting cover from potential exterior damaging actions and assures high anchoring capacity, overcoming some of the weaknesses of externally bonded systems [3, 5]. However, the widespread application of NSM FRP reinforcements is often limited by the scarcity of standards, procedures and methods to assess the quality of installations.

It is largely accepted that the performance of NSM FRP systems strongly depends on the mechanical properties of the epoxy adhesive [6, 7]. The initial fluid-like behaviour of the adhesive enables the correct application into the grooves, whereas this material gradually transforms into a rigid solid glass with significant strength as the polymerization reaction proceeds. This overall process, leading to a glassy polymer from a liquid low molecular weight mixture, is indicated in the literature as curing [8]. Various experimental research works have shown that the evolution of the tensile properties of epoxy adhesives is strongly dependent on environmental curing conditions, especially temperature [9-11]. Lower curing temperatures considerably decelerate the curing process and consequently the rate of the development of mechanical properties. In addition, some researchers [6, 12] have studied the evolution of the interface behaviour between FRP and concrete under different curing temperatures, reaching similar conclusions: the strength of an adhesive bond is critically dependent on curing time and temperature. While in industrial curing processes of epoxy resins, the temperature is a controlled variable that can be exactly set, such control is not

possible when the curing takes place in external environment, as is the case with most in-situ NSM FRP applications.

From the above considerations it is clear that monitoring of the curing process is of utmost importance in order to: (i) identify the time at which the material satisfies the minimum structural requirements (especially important in the case of pre-stressed systems [13]), as well as knowing the stiffness increase along time; (ii) confirm the adequate properties of the epoxy and its adequate mixing; (iii) be able to know when the epoxy assures the necessary mechanical properties that allow a strengthened element to operate in service conditions. Therefore, adequate non-destructive testing (NDT) approaches are required, in view of obtaining continuous information correlated to the curing of epoxy resins. Several NDT techniques have been proposed so far to monitor the curing process of epoxy resins, mainly resonant frequency-based methods [14-16], ultrasound techniques [17, 18], fibre-optic sensors (FOs) [19] and Raman spectroscopy [20].

The most used resonant frequency-based methods are the impulse excitation technique (IET) [14, 16] and the dynamic mechanical analysis (DMA) [15]. Both these methods require a mechanical shock to produce an excitation and therefore it is clear that these techniques are inadequate to monitor the curing process since the epoxy resin still has 'fluid-like' behaviour. Moreover, some researchers have raised repeatability concerns when DMA is applied to polymers [15, 21]. Alternatively, ultrasound techniques can provide continuous evaluation of the dynamic elasticity modulus of the epoxy resin right after mixing, measuring the velocity of propagation in the sample of generated ultrasonic waves [17, 18]. Although these wave-based methods allow overcoming some of the drawbacks of the conventional techniques based on the resonance frequency, the ultrasonic methods partially fail when material homogeneity is lacking (as the case of epoxy resin) and present some limitations due to the signal interpretation ambiguities of the received waves [17, 22]. A technique based on the use of FOs embedded through the reinforcing fibres of the FRP laminates was proposed by Antonucci *et al.* [19]. This method allows monitoring the advancement of the curing reaction of the resin, through measurement of the variation of the polymer density as a

consequence of polymerization. However, the cost of the equipment is still high and the optical fibres are susceptible to damage during installation in construction activities [23]. Raman spectroscopy is an efficient technique for the analysis of epoxy resins during cure because it detects chemical bonds and their changes during reaction and has an excellent time resolution. Nonetheless, it is an expensive technique and may have limited penetration depth depending on the characteristics of the material, such as refractive index and colour [24].

In concern to the study of concrete curing, a variant of the classical resonant frequency methods was proposed by Azenha *et al.* [25] for continuously monitoring the E-modulus evolution of concrete immediately after casting. Such experimental method has also been applied to cement pastes, mortars and stabilized soils [26, 27]. This technique, called Elasticity Modulus Measurement through Ambient Response Method (EMM-ARM), is a NDT method based on the identification of the first flexural resonant frequency of a composite beam that contains the material under testing. This natural frequency is then analytically related to the E-modulus of the material, which allows determining the evolution of this elastic property. The EMM-ARM can be easily deployed and applied for *in-situ* applications and overcomes the drawbacks of classical methods based on the resonance frequency, through two key differences: (i) the tested specimen never needs to be demoulded, whereby measurements can be initiated immediately after casting; and, (ii) identification of the resonance frequency is based on the ambient vibration, therefore no external forced excitation needs to be exerted on the specimen.

The present paper contributes to the definition of a non-destructive methodology for the quality control of NSM strengthening applications, based on the *in-situ* monitoring of the elastic modulus of epoxy adhesive. A simultaneous study of direct pull-out tests on concrete specimens strengthened with NSM CFRP laminate strips was conducted since early ages. The relationship between the evolution of epoxy E-modulus and the maximum pull-out force was assessed, evaluating the possibility of a correlation between these two entities, with relevant potential for the *in-situ* quality control. It is remarked that no reference could be

5

1 found in the literature concerning experimental studies that relate the epoxy E-modulus to the

2 maximum pull-out force of NSM systems.

3

4 **2   EXPERIMENTAL PROGRAMME**

5 The experimental work was composed of two parts: (i) EMM-ARM tests were performed for

6 monitoring the hardening process of a structural epoxy adhesive used in FRP applications;

7 (ii) direct pull-out tests with concrete specimens strengthened with NSM CFRP laminate

8 strips were carried out to assess the evolution of bond performance between CFRP and

9 concrete since early ages. In order to assess the capability of the EMM-ARM method for

10 evaluating the elastic modulus of the epoxy, static E-Modulus was determined through

11 tension tests, carried out according to ISO 527-2:2012. The experimental procedures were

12 performed in a climatic chamber under controlled environmental conditions, with temperature

13 (T) of 20±1ºC and relative humidity (RH) of 60±5%.

14

15 **2.1   Materials and characterization**

16 This section presents the characterization of the materials involved in this experimental

17 programme at a matured state, namely concrete, CFRP laminate strip and epoxy adhesive.

18 The pull-out tests were carried out on concrete cubic specimens (200 mm edge) that were

19 three years old at the date of this experimental programme. The mechanical characterization

20 of concrete in terms of compressive strength and Young modulus was carried out through

21 compression tests performed on concrete cylindrical cores (200 mm height, 100 mm

22 diameter), in accordance to EN 12390-3:2009 and LNEC E397-1993:1993, respectively. The

23 obtained results showed an average compressive strength, f_{cm} of 42.35 MPa, with a

24 coefficient of variation CoV of 5.22%, and an average Young's modulus, E_{cm} of 38.25 GPa

25 (CoV=8.38%).

26 The CFRP laminate used in this experimental research, with a cross-sectional area of 1.4×10

27 mm^2, was produced by S&P® Clever Reinforcement (trademark: *CFK 150/2000*) and

28 provided in rolls. This laminate consists of unidirectional carbon fibres held together by an

6

epoxy vinyl ester resin, and presents a smooth surface. The evaluation of mechanical properties of this CFRP laminate was performed according to ISO 527-5:2009. From six tested specimens, a Young's modulus, a tensile strength and a strain at peak stress of 169.5 GPa (CoV=2.5%), 2648.3 MPa (CoV=1.8%) and 1.6% (CoV=1.8%) were obtained, respectively.

The epoxy adhesive used in the experimental work, produced by the same supplier of CFRP material, had the trademark *S&P Resin 220 epoxy adhesive®*. This epoxy adhesive is a solvent free, thixotropic and grey two-component (Component A = resin and Component B = hardener). The hardener to epoxy volumetric ratio was 1:4 as suggested by the supplier. To characterize the epoxy adhesive, four tensile tests were carried out, in accordance to ISO 527-2:2012 recommendations. The mixture used for making these epoxy specimens was the same used for the pull-out and EMM-ARM tests. After casting, the four specimens were cured and kept in the climatic chamber for ten days before being tested. The average stress-strain curve of the performed tensile tests is presented in Figure 1. For each specimen the Young's modulus was obtained by two different methods: (i) the first tensile modulus, E_{std}, was calculated as the slope of the secant line between 0.05% and 0.25% strain on the stress-strain plot, according to ISO 527-1:2012; (ii) the second, E_{inslop}, represents the slope of the linear trend line of the experimental values gathered until 1/3 of the ultimate strength, according to the American Standard ASTM D638M-93. From the tests an average tensile strength of 21.98 MPa (CoV=0.87%), E_{std} of 7.10 GPa (CoV=5.74%) and a strain at the peak stress of 0.40 MPa (CoV=8.13%) were obtained. The average modulus calculated by the trend line method (E_{inslop}) turned out to be 8.22 GPa (CoV=18.94%), 15.8% larger than the secant modulus (E_{std}).

2.2 EMM ARM Tests

In order to adapt EMM-ARM to the study of epoxy adhesive used in NSM CFRP applications, some alterations were necessary in regard to the previous applications of this method to the

study of cement pastes on which it is based [27]. This section provides a brief outline of the experimental setup and procedure

In the applications of the present work, the EMM-ARM specimen consists in a cantilever beam where the accelerations are monitored at its free end. The adopted experimental setup is reproduced in Figure 2. The mould consists of a 330 mm long acrylic tube with inside/outside diameters of 16/20 mm. Firstly the epoxy adhesive to be tested is injected inside the acrylic tube through a 100 ml syringe. Then, after closing both extremities with two propylene caps, the composite cylinder is rigidly connected to a heavy steel profile through a metal clamping device, ensuring the structural behaviour of a cantilever beam. Due to a clamping length of 80 mm, the cantilevered part of the beam has a total span of L=250 mm. Finally, a lightweight accelerometer (PCB 352A10 with mass of 5.8 g; sensitivity 100 mV/g; frequency range: 0.5 to 10000 Hz) is glued at the free end extremity of the cantilever, in order to monitor accelerations in the vertical direction induced by ambient excitation (e.g.: people walking nearby; room ventilation; vibrations produced by mechanical equipment). Concerning technical specifications of the data acquisition system, a 24 bit dynamic signal acquisition module NI USB-9233 connected to a PC was used. The ambient vibrations were increased by placing a domestic fan pointing at the samples, thus increasing the amplitude of the measured accelerations and facilitating the modal identification. The monitored process started immediately after placement of the accelerometer, which occurred within ~20 minutes since the epoxy components started to be mixed. Accelerations were recorded in sets of 300 seconds, acquired at intervals of 600 seconds and a frequency of 1000 Hz. Then, the recorded accelerations were converted to the frequency domain, using the Welch procedure [28]. The detailed explanation of the whole modal identification process is provided in reference [27]. The resonant frequencies of the composite cantilever beam were identified for each of 300 seconds period of testing through the highest peak in the amplitude spectrum. Based on the dynamic equation of free vibration together with full information about the geometry and mass of the system, and knowledge of the stiffness properties of the acrylic tubes, the E-modulus of the epoxy adhesive could be determined along time.

1   In order to evaluate the method's ability to obtain results with good repeatability, two tests

2   were performed simultaneously (EMM1 and EMM2). The acrylic tubes used for the EMM-

3   ARM experiments had an average elastic modulus of 4.27 GPa at 20ºC (with a variation of

4   ±0.13 GPa) and an average density of 1225.9 kg/m^3 (with a variation of ±13.6 kg/m^3). The

5   values of E-modulus and density of the acrylic were assessed in the laboratory through

6   modal identification of the empty molds, which were weighed before each test. The

7   geometric characteristics of the molds, as well as the density of the epoxy adhesive, are

8   shown in Table 1. An important issue has to be remarked: at the end of each EMM-ARM test

9   the composite cantilever was sawn into eight parts for carefully checking the possible

10   formation of air bubbles inside the tested material or even acrylic/epoxy debonding. In fact,

11   the non-fulfilment of the uniform mass distribution along the tube, or lack of full bond within

12   the composite section, may affect the applicability of the analytical formulation for calculation

13   of the E-modulus of the epoxy. None of such situations were observed in the tested

14   specimens.

15

16   **2.3   Direct pull-out tests**

17   The geometry and the configuration adopted for the monotonic direct pull-out tests are

18   shown in Figure 3. The specimen consisted of a concrete cubic block of 200 mm edge, into

19   which a CFRP laminate strip with 1.4 mm thickness and 10 mm width was embedded. The

20   depth and the width of the groove for insertion of the CFRP laminate strip were, respectively,

21   15 mm and 5 mm. The bond length, filled with the epoxy adhesive, was 60 mm. To avoid a

22   premature splitting failure in the concrete ahead of the loaded-end, the bond length started

23   100 mm away from the top of the block. A steel plate of 20 mm thickness was applied on top

24   of the concrete cube in order to ensure negligible vertical displacement during the test. The

25   plate was fixed to the support base by means of four M10 steel threaded rods. A torque of

26   30 N×m was applied, inducing an initial compression to concrete of ~2.0 MPa. The pull-out

27   tests were performed on a closed steel frame equipped with a servo-controlled equipment.

28   The applied force, F, was measured with a load cell of 200 kN of maximum carrying capacity

1   (with a linearity error less than ±0.05% F.S.) placed between the load actuator and the grip.

2   A LVDT displacement transducer (range ±2.5 mm with a linearity error of ±0.05% F.S.) was

3   used to measure the slip at the loaded end. The tests were undertaken under displacement

4   control through a transducer placed between the grip and the actuator, at a rate of 2 μm/s.

5   The preparation of the strengthened specimens required several steps. Firstly, grooves were

6   made in each concrete cube, using a saw cutting machine with diamond blade. To obtain the

7   actual geometry of the grooves, two measurements of their depth and width were carried out

8   for each specimen, using a digital calliper with an accuracy of ±0.01 mm. The obtained

9   average values of depth and width of the grooves are respectively, 14.13 mm (CoV = 2.66%)

10 and 5.21 mm (CoV = 2.92%). The reinforcement of the specimens was carried out about 30

11 days after the grooves were made on the cubes. During this period, all the components

12 (grooved concrete blocks, CFRP laminates and epoxy adhesive components) were kept in

13 the climatic chamber at T=20±1ºC RH=60±5%. Before strengthening, the grooves were

14 cleaned with compressed air. For each specimen, after mixing the two components of the

15 adhesive, the groove was filled with epoxy. Then the CFRP laminate was carefully inserted

16 into the groove and, finally, the surface was levelled. After strengthening, the specimens

17 were kept in the previously described climatic chamber environment until the age of testing.

18 The experimental programme was composed by twenty validated pull-out bond tests at

19 several ages. The first test was carried out 6 hours after epoxy mixing. During the initial

20 period, more frequent tests were scheduled, to accurately assess the evolution of bond

21 behaviour since early ages. Therefore, the specific testing times were 6, 9, 12, 24, 36, 48,

22 72, 168, 336 hours, 30 days and 3 months. For each age of testing (except 6 and 9 hours) it

23 was decided to perform two consecutive tests as close as possible, to ensure that the results

24 could be confirmable. The generic denomination of each specimen, relevant in the scope of

25 presentation of results in Table 2, is DPTX_Y, where X is the specimen number (1, 2,..., 20)

26 and Y is the testing time (6h, 9h,..., 336h, 30d and 3m).

27

3 RESULTS AND DISCUSSON

In the following sections the results of the experimental work are presented, beginning with the EMM-ARM results followed by the results of the direct pull-out tests. After separately showing and discussing the outcomes of the two test series, a comparison between the E-Modulus evolution of the epoxy adhesive and the pull-out force is presented.

3.1 EMM-ARM test results

The frequency spectra obtained for specimen EMM1 at several ages (1, 8, 17 and 134 hours) are shown in Figure 4. From this figure, it is possible to clearly evaluate the resonant frequency at the presented ages, as the corresponding peaks are quite easily distinguishable and no relevant secondary peaks are observed in the frequency range of interest.

The evolution of first resonant frequencies of EMM1 and EMM2 is shown in Figure 5a. It is worth mentioning that a wide range of frequencies was covered throughout the curing process of the adhesive (from ~49.9 Hz to ~77.8 Hz within the test period), allowing a good resolution for the E-modulus identification.

After determining the resonant frequency of each composite beam, the elasticity modulus of the tested epoxy adhesive was inferred by applying the vibration equation of a cantilevered structural system, as seen in [27]. Table 1 shows the measured characteristics of the EMM-ARM specimens which were used for the calculation. The resulting E-modulus evolution for both specimens is shown in Figure 5b. Firstly, it is possible to verify the good agreement between the results of the two specimens, with absolute stiffness differences always remaining under 2.2%, revealing the good repeatability of the experimental setup and procedure. During the first 6.45 hours the epoxy stiffness was nearly null for both specimens, which is consistent with the fluid-like behaviour of the adhesive at the early stages of the curing. Then a drastic increase in the stiffness occurred, reaching an average value of ~8.6 GPa at the age of 35 hours, instant after which the E-modulus evolution reached a plateau during the following 109 hours. In fact the final values at the end of testing (144 hours) were 8.94 GPa and 8.86 GPa for EMM1 and EMM2, respectively.

1   Figure 5b also shows the elastic modulus values (E_{std}=7.10 GPa and E_{inslop}=8.22 GPa)

2   obtained by tensile tests at the age of 10 days. These two values fall within feasible ranges

3   (6.36-8.68 GPa) in view of reported results in the literature for similar epoxies [29, 30]. A

4   comparison of E-modulus obtained by EMM-ARM and through tensile tests shows a non-

5   negligible difference: the last average value of E-modulus monitored by EMM-ARM at the

6   age of ~144 hours is much higher than the value E_{std} determined by ISO 527-1:2012 at the

7   age of 240 hours, with a difference of about 1.80 GPa (20.2%). There are fundamental

8   differences between EMM-ARM testing and the tensile testing involved in the determination

9   of E_{std} and E_{inslop}: (i) strain rates are distinct; (ii) stress levels are different; (iii) the duration of

10   each loading/testing is not the same. Therefore, particularly due to issues (ii) and (iii), it is

11   plausible to infer that the E-modulus estimated by EMM-ARM may possibly result in higher

12   values than those obtained thorough E_{inslop}. Indeed the stress level of EMM-ARM is lower,

13   and creep effects during EMM-ARM testing are surely less important [31]. However, when

14   comparing EMM-ARM values with the E-modulus E_{inslop} calculated from the initial slope of

15   monotonic stress-strain curves, it should be noted that the difference between them is

16   significantly lower (0.68 GPa – a difference of 7.6%) and can be considered reasonable. This

17   is a good indication regarding the capability of EMM-ARM in clearly evaluating the values of

18   static E-modulus of epoxy adhesives. Moreover, the described results demonstrate the

19   suitability of this technique for monitoring the stiffness evolution of the tested material, thus

20   offering interesting opportunities for the quality control of the curing of epoxy resins.

21   For the description of the results, two different mathematical models are presented. Since the

22   curing reactions of the epoxy material are autocatalytic, a corresponding logistic equation

23   may be employed, according to Gershenfeld [32]. The equation takes the following form:

$$E(t) = \frac{E_0 - E_\infty}{1 + (t / t_m)^s} + E_\infty \qquad (1)$$

24   where $E(t)$, E_0 and E_∞ are the E-modulus values at a given time, t, at the beginning ($t = 0$)

25   and at the end of the curing process, respectively. The parameter t_m is the time required to

1   attain a value of $E_\infty / 2$ and *s* represents the reaction rate, governing the slope of the curve.

2   The value E_0 was assumed zero for freshly mixed material, while the E-modulus end value,

3   E_∞, is the average of experimental values at the end of testing (8.90 GPa). The parameter *s*

4   was determined by regression of test results (*s*=3.582). A good agreement between

5   experimental and modelling results was found (with a coefficient of determination

6   R^2=0.9974), as shown in Figure 6. However, the Gershenfeld model fails to capture the real

7   behaviour of the epoxy adhesive at the beginning of the curing. In order to obtain a better

8   mathematical model describing the early-age development of epoxy E-modulus, the equation

9   proposed by Silva *et al.* [26] was used. This model is based on existing approaches for the

10   stiffness evolution prediction of concrete [33] and expresses the elastic modulus by the

11   following equation:

$$E(t) = E_\infty \exp\left[-\frac{1}{2}\left(\frac{\tau}{t}\right)^\beta \right] \tag{2}$$

12   where *β* is the reaction shape parameter and *τ* is the reaction time parameter. Regression

13   analyses were performed to determine these parameters, using experimental values: (*β, τ*) =

14   (2.779; 12.926). The best fit was achieved using the method of least squares, in order to

15   maximize the coefficient of determination between the model and the experimental curve. By

16   observing Figure 6, it is possible to verify that the use of Equation (2) allows to obtain a very

17   good estimate of E-modulus evolution (R^2=0.9995), even at the early stages of the curing.

18

19   **3.2   Pull-out test results**

20   The main results of the monotonic pull-out tests are summarized in Table 2. In order to

21   assess the evolution of bond performance, the following parameters were analyzed: the

22   maximum pull-out force, $F_{l,max}$; the ratio between $F_{l,max}$ and CFRP tensile strength, F_{fu}; the slip

23   at the loaded end at $F_{l,max}$, $s_{l,max}$; the average bond strength at the CFRP-epoxy interface, τ_{max}

24   that is evaluated by the expression $F_{l,max}/(P_f L_b)$, where P_f is the perimeter of the CFRP cross-

25   section in contact with the adhesive and L_b is the bond length. Table 2 also provides

1   Information about the failure mode of the experiments, with the following codes:

2   D=debonding at CFRP-epoxy interface; FE=cohesive shear failure in epoxy; CC=concrete

3   cracking; SE=splitting of epoxy.

4   As Table 2 shows, cohesive shear failure in the adhesive (FE) occurred at the early ages

5   until 12 hours, confirming the low mechanical properties of the adhesive at the beginning of

6   the curing (see Figure 7b). This was to be expected in view of previous experimental findings

7   [34, 35]. In fact the pure interfacial failure is critical for bars with a smooth surface [3]: since

8   the smooth surface of CFRP strips is insufficient to provide mechanical interlocking between

9   the laminate and the adhesive, and the rougher surface of the concrete leads to better

10   bonding with the adhesive, the bond resistance relies primarily on chemical adhesion

11   between the strip and the epoxy. Moreover, the tests performed at 36 and 73 hours also led

12   to cracking of the epoxy cover and fracture in the concrete along inclined planes (SE+CC -

13   see Figure 7c).For the specimen tested at 48 hours, concrete cracking with no visible

14   splitting of epoxy was observed (CC). In fact, although the tensile strength of epoxy was

15   much higher than that of concrete, the very small epoxy thickness could lead to the splitting

16   of adhesive cover due to the formation of a resistant strut and tie mechanism described by

17   Sena *et al.* [36].

18   Figure 8 shows the relationship between the pull-out force and slip at loaded end ($F_l – s_l$) of a

19   selected group of significant tested specimens. The figure shows the increase in bond

20   stiffness and strength along the curing period of the epoxy adhesive. This evolution process

21   seems to be highly controlled by the state of hardening of the adhesive. At the age of 6

22   hours, since the epoxy has not yet begun to harden, the pull-out force remains approximately

23   null, with a maximum of 0.2 kN. From 6 to 24 hours the bond stiffness has a significant

24   increase, showed by the sharp slope difference of the curves obtained by the tests

25   performed at 9, 12 and 24 hours. As Figure 8 shows, this variation in the shape of the curves

26   is consistent with the different failure modes observed at the early ages (identified by a

27   shadowed region labelled as 'FE' in Figure 8). At the age of 24 hours, the $F_l – s_l$ curves start

28   exhibiting the characteristic bond-slip behaviour observed at testing ages such as 3 months,

1 when the epoxy has achieved a significant maturity level. These $F_l – s_l$ curves initially show

2 an almost linear branch due to the chemical bond existing between adhesive and CFRP.

3 When this bond starts to be damaged, the response becomes non-linear up to the peak pull-

4 out load. The failure finally occurs after a short post-peak descending branch.

5 Figure 9 depicts the evolution of the peak pull-out force ($F_{l,max}$) and the corresponding slip at

6 the loaded end ($s_{l,max}$) during the curing process. It could be noted that $F_{l,max}$ results null at 6

7 hours, showing that the epoxy has not yet any relevant stiffness nor strength. $F_{l,max}$ has a

8 significant increase from 6 to 24 hours when the maximum value is reached. Between 6 and

9 9 hours the peak pull-out force increases by 3 kN and even by 10.56 kN in the subsequent 4

10 hours. The maximum pull-out force reaches a constant value of 24.9 kN with a variation of ±

11 1.28 kN (5.13%) after 24 hours. As expected, the loaded end slip $s_{l,max}$ was much higher

12 during the early hours, due to the fact that the epoxy was not yet completely hardened. After

13 the first 24 hours the $s_{l,max}$ remained at a plateau value of 0.65 mm ±11.5 %. To summarize,

14 the pull-out tests revealed that: (i) from 6 to 24 hours after strengthening of the specimens,

15 the bond stiffness had an important increase; (ii) from 24 hours to 3 months, the bond

16 stiffness did not show any significant variation.

17

18 **3.3 Comparison between the evolution of epoxy E-modulus and the maximum pull-**

19 **out force along time**

20 In order to verify the relationship between the bond behaviour of NSM systems and epoxy E-

21 modulus, a comparison between the peak pull-out force and the E-modulus of the same

22 epoxy mixture used for strengthening the pull-out specimens is carried out, as shown in

23 Figure 10a. From this figure it can be noted that the results of both experimental techniques

24 exhibit very similar evolution kinetics. In regard to the beginning of the setting of the epoxy

25 adhesive, there is a good coherence between E-modulus and pull-out force. Moreover, the

26 increase of the bond stiffness is consistent with the stage at which the curing reactions of

27 epoxy are in progress. Thus, it is possible to obtain a correlation between the E-modulus and

28 pull-out force, as shown in Figure 10b. This figure highlights that the evolution of the epoxy

adhesive E-modulus seems to exhibit a slightly more accelerated evolution kinetics than the pull-out force during the phase of higher reaction of the epoxy adhesive. Despite that, it is clear that the bond performance of NSM CFRP systems is strongly related to the stiffness (and hence the mechanical properties in general) of the epoxy resins. Therefore, the availability of a technique such as EMM-ARM, providing continuous and quantitative information about the stiffness of the epoxy adhesive, offers interesting opportunities for quality control and in-situ monitoring of NSM FRP applications, estimating the minimum curing time to reach a threshold value of pull-out force. Moreover, it is noteworthy to mention the clear ability of the EMM-ARM technique to identify the instant at which thermosetting reactions begin, and stiffness starts developing at a fast rate. EMM-ARM results also allowed a clear identification of the early curing kinetics and the instant at which stiffness development rate suffers an intense deceleration. The structural setting time, as well as the early evolution of stiffness, are important parameters to actually determine when epoxy starts to hold stresses and represent information of paramount importance in order to know the time required to put the strengthened structure in service.

4   CONCLUSIONS

The present paper described the application of EMM-ARM for monitoring of the stiffening of an epoxy adhesive used in NSM FRP strengthening applications. A simultaneous study comprising direct pull-out tests with concrete specimens strengthened with NSM CFRP laminate strips was carried out to compare the evolution of bond performance with the epoxy E-modulus since early ages. The main conclusions of the study can be summarized as follows:

1. EMM-ARM confirmed its capability in clearly identifying the hardening kinetics of epoxy adhesives, measuring the material setting time and the stiffness growth since very early ages;

2. the obtained stiffness evolution of epoxy demonstrated a good repeatability of EMM-ARM;

3. two analytical models were used for describing the development of epoxy E-modulus during the curing period. Modelling and experimental EMM-ARM results compared well, opening interesting opportunities for design purposes and for the prediction of the final stiffness over time;

4. the bond behaviour of concrete elements strengthened with NSM CFRP laminate strips was assessed since the early age of the epoxy curing and a significant evolution of maximum pull-out force was observed in the first 24 hours of the epoxy curing, after which the force evolution tends to become stagnant;

5. the peak pull-out force and the epoxy E-modulus obtained by EMM-ARM exhibit very similar evolution kinetics, thus indicating that the bond performance of NSM CFRP system strongly depends on the stiffness of the epoxy resin.

Concerning its applications, EMM-ARM can be employed for in-situ monitoring of the hardening of an epoxy adhesive curing in un-controlled conditions, as may be those of a construction site, as basis for decisions concerning the duration of construction stages or waiting periods prior to putting strengthened structures into service. Consequently, it is plausible to use the EMM-ARM for quality control and assistance to decision-making for the NSM FRP reinforcement technique. Moreover, EMM-ARM can be used to assist the study of the effects of curing temperature and curing time on the mechanical properties of epoxy adhesives or even to study the degradation of the mechanical properties due to severe environmental conditions that the reinforced structures may suffer over time.

REFERENCES

[1] Teng JG, Chen J-F, Smith ST, Lam L. FRP: strengthened RC structures. Frontiers in Physics. 2002;1.

[2] Bakis C, Bank LC, Brown V, Cosenza E, Davalos J, Lesko J, et al. Fiber-reinforced polymer composites for construction-state-of-the-art review. Journal of Composites for Construction. 2002;6(2):73-87.

[3] De Lorenzis L, Teng JG. Near-surface mounted FRP reinforcement: An emerging technique for strengthening structures. Composites Part B: Engineering. 2007;38(2):119-43.

[4] De Lorenzis L, Nanni A. Characterization of FRP rods as near-surface mounted reinforcement. Journal of Composites for Construction. 2001;5(2):114-21.

[5] Sena-Cruz JM, Barros JAO, Coelho MR, Silva LF. Efficiency of different techniques in flexural strengthening of RC beams under monotonic and fatigue loading. Construction and Building Materials. 2012;29:175-82.

[6] Czaderski C, Martinelli E, Michels J, Motavalli M. Effect of curing conditions on strength development in an epoxy resin for structural strengthening. Composites Part B: Engineering. 2012;43(2):398-410.

[7] Borchert K, Zilch K. Bond behaviour of NSM FRP strips in service. Structural Concrete. 2008;9:127-42.

[8] Gillham JK. Formation and properties of thermosetting and high Tg polymeric materials. Polymer Engineering & Science. 1986;26(20):1429-33.

[9] Matsui K. Effects of curing conditions and test temperatures on the strength of adhesive-bonded joints. International Journal of Adhesion and Adhesives. 1990;10(4):277-84.

[10] Moussa O, Vassilopoulos AP, de Castro J, Keller T. Early-age tensile properties of structural epoxy adhesives subjected to low-temperature curing. International Journal of Adhesion and Adhesives. 2012;35:9-16.

[11] Lapique F, Redford K. Curing effects on viscosity and mechanical properties of a commercial epoxy resin adhesive. International Journal of Adhesion and Adhesives. 2002;22(4):337-46.

[12] Dutta PK, Mosallam A. A rapid field test method to evaluate concrete composite adhesive bonding. International Journal of Materials and Product Technology. 2003;19(1):53-67.

[13] Michels J, Sena-Cruz J, Czaderski C, Motavalli M. Structural Strengthening with Prestressed CFRP Strips with Gradient Anchorage. Composites for Construction. 2013;17(5):651-61.

[14] Schmidt R, Alpern P, Tilgner R. Measurement of the Young's modulus of moulding compounds at elevated temperatures with a resonance method. Polymer Testing. 2005;24(2):137-43.

[15] Deng S, Hou M, Ye L. Temperature-dependent elastic moduli of epoxies measured by DMA and their correlations to mechanical testing data. Polymer Testing. 2007;26(6):803-13.

[16] Tognana S, Salgueiro W, Somoza A, Marzocca A. Measurement of the Young's modulus in particulate epoxy composites using the impulse excitation technique. Materials Science and Engineering: A. 2010;527(18–19):4619-23.

[17] Lionetto F, Maffezzoli A. Monitoring the Cure State of Thermosetting Resins by Ultrasound. Materials. 2013;6(9):3783-804.

[18] Frigione M, Maffezzoli A, Acierno D, Luprano VAM, Montagna G. Nondestructive and in-situ monitoring of mechanical property buildup in epoxy adhesives for civil applications by propagation of ultrasonic waves. Polymer Engineering & Science. 2000;40(3):656-64.

[19] Antonucci V, Giordano M, Prota A. Fiber Optics Technique for Quality Control and Monitoring of FRP Installations. FRPRCS-7. Kansas City, USA: American Concrete Institute; 2005. p. 195-207.

[20] Merad L, Cochez M, Margueron S, Jauchem F, Ferriol M, Benyoucef B, et al. In-situ monitoring of the curing of epoxy resins by Raman spectroscopy. Polymer Testing. 2009;28(1):42-5.

[21] Lee-Sullivan P, Dykeman D. Guidelines for performing storage modulus measurements using the TA Instruments DMA 2980 three-point bend mode: I. Amplitude effects. Polymer Testing. 2000;19(2):155-64.

[22] Challis RE, Blarel F, Unwin ME, Paul J, Guo X. Models of ultrasonic wave propagation in epoxy materials. Ultrasonics, Ferroelectrics and Frequency Control, IEEE Transactions on. 2009;56(6):1225-37.

[23] Li H-N, Li D-S, Song G-B. Recent applications of fiber optic sensors to health monitoring in civil engineering. Engineering Structures. 2004;26(11):1647-57.

[24] Hardis R, Jessop JLP, Peters FE, Kessler MR. Cure kinetics characterization and monitoring of an epoxy resin using DSC, Raman spectroscopy, and DEA. Composites Part A: Applied Science and Manufacturing. 2013;49(0):100-8.

[25] Azenha M, Magalhães F, Faria R, Cunha Á. Measurement of concrete E-modulus evolution since casting: A novel method based on ambient vibration. Cement and Concrete Research. 2010;40(7):1096-105.

[26] Silva J, Azenha M, Correia AG, Ferreira C. Continuous stiffness assessment of cement-stabilised soils from early age. Geotechnique. 2013;63(16):1419-32.

[27] Azenha M, Faria R, Magalhães F, Ramos L, Cunha Á. Measurement of the E-modulus of cement pastes and mortars since casting, using a vibration based technique. Mater Struct. 2012;45(1-2):81-92.

[28] Welch PD. The use of fast Fourier transform for the estimation of power spectra: A method based on time averaging over short, modified periodograms. Audio and Electroacoustics, IEEE Transactions on. 1967;15(2):70-3.

[29] Sena-Cruz JM, Michels J, Czaderski C, Motavalli M, Castro F. Mechanical behavior of epoxy adhesives cured at high temperatures, Report no. 880163. Empa, Swiss Federal Laboratories for Materials Science and Technology, Switzerland; 2012. p. 40.

[30] Costa I, Barros JAO. Assessment of the long term behaviour of structural adhesives in the context of NSM flexural strengthening technique with prestressed CFRP laminates. FRPRCS11. Guimarães, Portugal2013.

[31] Shen X, Xia Z, Ellyin F. Cyclic deformation behavior of an epoxy polymer. Part I: Experimental investigation. Polymer Engineering & Science. 2004;44(12):2240-6.

[32] Gershenfeld N. The nature of mathematical modeling: Cambridge University Press; 1999.

[33] Krauss M, Rostàsy FS, Hariri K. Non-Destructive Assessment of Mechanical Properties of Concrete at Very Early Age by US Techniques – Method, Results and Modelling. Braunschweig, Germany: Institute for Building Materials, Concrete Construction and Fire Protection (IBMB), Technische Universitat Braunschweig; 2001. p. 34.

[34] Teng J, De Lorenzis L, Wang B, Li R, Wong T, Lam L. Debonding Failures of RC Beams Strengthened with Near Surface Mounted CFRP Strips. Journal of Composites for Construction. 2006;10(2):92-105.

[35] Blaschko M. Bond behaviour of CFRP strips glued into slits. Sixth International Symposium on FRP Reinforcement for Concrete Structures (FRPRCS-6): World Scientific; 2003. p. 8-10.

[36] Sena Cruz JM, Barros JAO. Bond between near-surface mounted carbon-fiber-reinforced polymer laminate strips and concrete. Journal of composites for construction. 2004;8(6):519-27.

1   **LIST OF TABLES**

2   Table 1 – Characteristics of EMM-ARM specimens

3   Table 2 – Pull-out test results.

4

1   Table 1 – Characteristics of EMM-ARM specimens

Reference	L [mm]	$\varnothing_e$ [mm]	$\varnothing_i$ [mm]	M_{Accel} [g]	ρ_{Acryl} [kg/m^3]	ρ_{Epoxy} [kg/m^3]
EMM1	250	20.099	15.975	7.07	1239.49	1702.98
EMM2	250	20.086	16.030	7.06	1212.27	1749.43

2   Notes: L is the free span; $\varnothing_e$ and $\varnothing_i$ are, respectively, the external and the internal diameter of the
3   acrylic tube; M_{Accel} is the mass of the accelerometer; ρ_{Acryl} is the density of the acrylic tube; ρ_{Epoxy} is the
4   density of the epoxy.

1   Table 2 – Pull-out test results.

Time	Real testing time [h]	Reference	$F_{l,max}$ [kN]	$F_{l,max}$ / F_{fu} [%]	τ_{max} [MPa]	$s_{l,max}$ [mm]	Failure mode
6h	5.9	DPT1_6h	0.02	0.06	0.01	-	FE
9h	8.9	DPT2_9h	3.07	8.77	2.24	0.97	FE
12h	11.2	DPT3_12h	9.11	26.03	6.66	1.64	FE (Figure 7a)
	12.8	DPT4_12h	13.63	38.94	9.96	1.27	FE
24h	24.5	DPT5_24h	26.27	75.06	19.20	0.64	D
	25.9	DPT6_24h	25.76	73.60	18.83	0.55	D
36h	36.9	DPT7_36h	25.32	72.34	18.51	0.69	D+SE+CC (Figure 7c)
	38.1	DPT8_36h	23.83	68.09	17.42	0.63	D
48h	49.0	DPT9_48h	23.29	66.54	17.02	0.65	D+CC
	49.9	DPT10_48h	26.24	74.97	19.18	0.68	D
72h	72.2	DPT11_72h	26.17	74.77	19.13	0.72	D
	73.2	DPT12_72h	27.24	77.83	19.91	0.68	D+SE+CC
168h	168.6	DPT13_168h	24.50	70.00	17.91	0.49	D
	169.9	DPT14_168h	23.87	68.20	17.45	0.56	D (Figure 7b)
336h	338.3	DPT15_336h	24.41	69.74	17.84	0.73	D
	339.5	DPT16_336h	23.84	68.11	17.43	0.69	D
30d	721.9	DPT17_30d	-	-	-	-	-
	727.2	DPT18_30d	22.88	65.37	16.73	0.57	D
3m	2260.7	DPT19_3m	24.27	69.34	17.74	0.67	D
	2261.7	DPT20_3m	25.48	72.80	18.63	0.75	D

2   Notes: FE=cohesive shear failure in epoxy; D=debonding at CFRP-epoxy interface; CC=concrete
3   cracking; SE=splitting of epoxy;

23

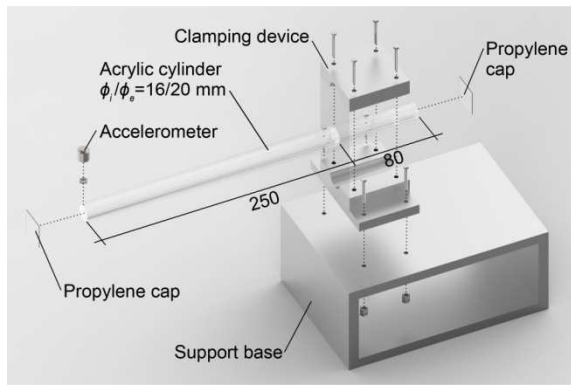1 **LIST OF FIGURES**
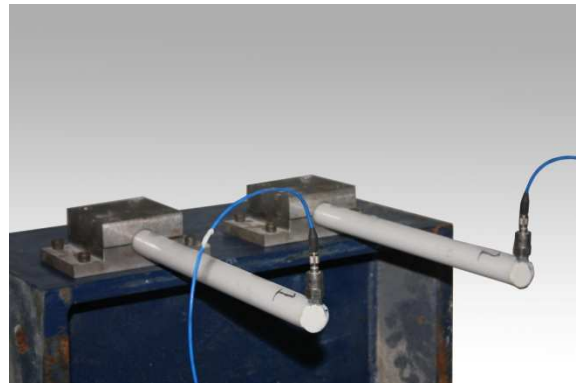
18

19

1

2   Figure 1 – Stress-strain curve obtained from tensile tests of the epoxy adhesive

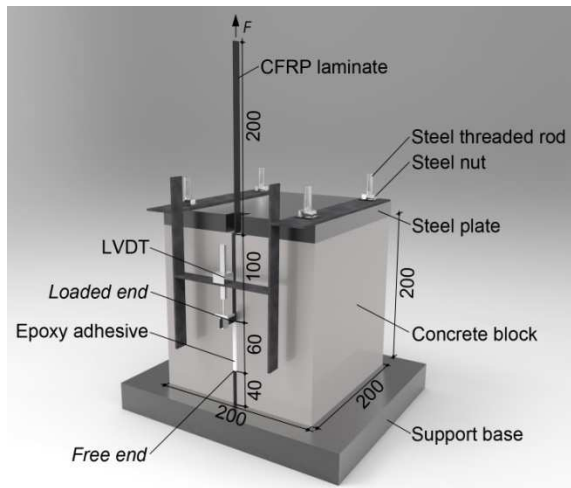(a)   (b)
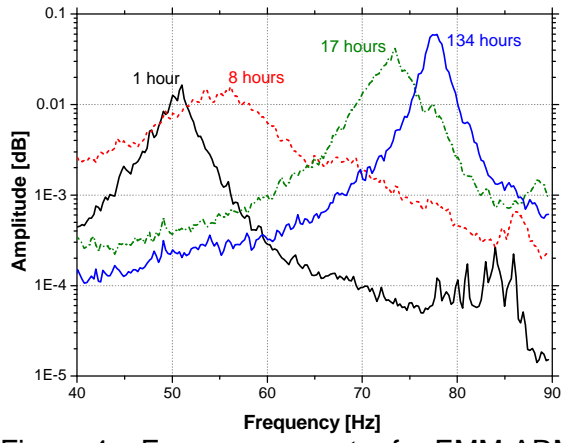
1   Figure 2 – Experimental setup of EMM-ARM tests: (a) exploded view [units: mm]; (b) photo
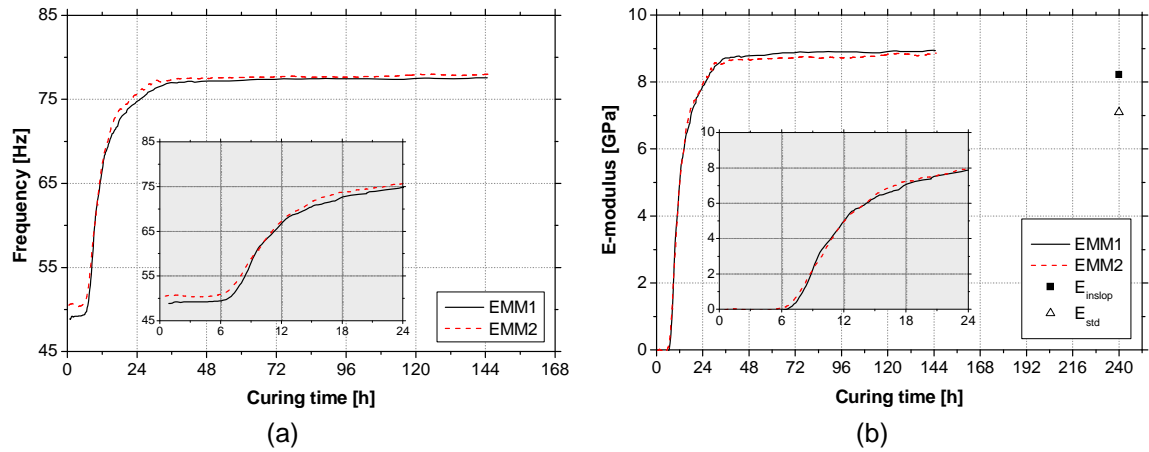
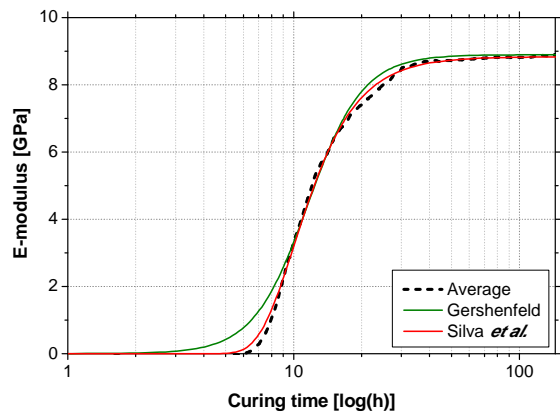(a)   (b)

1   Figure 3 – Direct pull-out test configuration: (a) geometry [units: mm]; (b) photo.

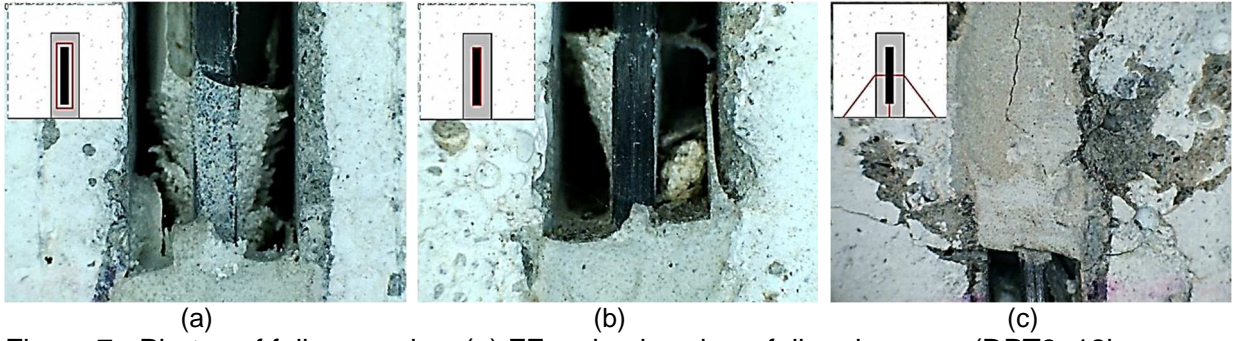Figure 4 – Frequency spectra for EMM-ARM beam EMM1 at different ages

(a)   (b)

Figure 5 – EMM-ARM results: (a) frequency evolution; (b) E-modulus evolution

Figure 6 – Average stiffness evolution obtained by EMM-ARM compared to mathematical models.

1

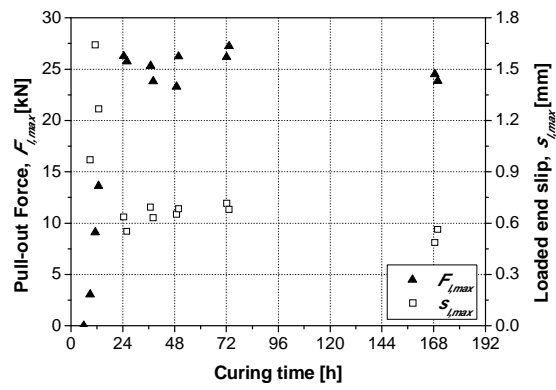(a)   (b)   (c)

Figure 7 - Photos of failure modes: (a) FE: cohesive shear failure in epoxy (DPT3_12h –
Loaded end region); (b) D: debonding at CFRP-epoxy interface (DPT14_168h - Loaded end
region); (c) SE+CC: cracking of the epoxy cover and fracture in the concrete (DPT7_36h –
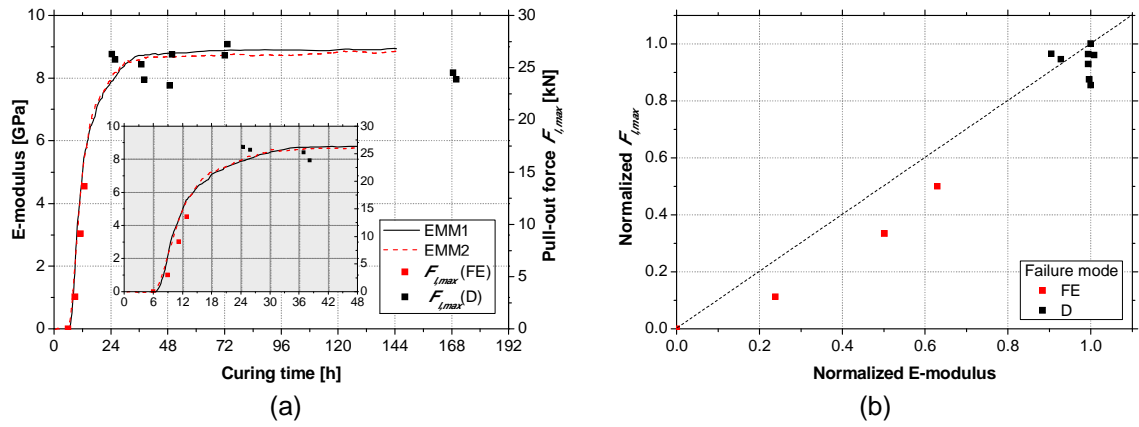Free end region).
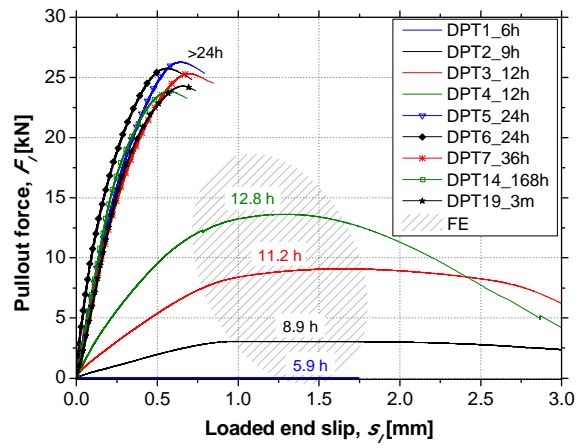
Figure 8 - Evolution of maximum pull-out force and corresponding loaded end slip during the curing time

1
2   Figure 9 – Pull-out force and loaded end slip as functions of curing time

(a)

(b)

1 Figure 10 – (a) Comparison between the evolution of the epoxy E-modulus and the pull-out
2 force along time; (b) Correlation between the epoxy E-modulus and the pull-out force